Efficient Hydrodesulfurization of Dibenzothiophene over Core-Shell Ni/Al 2 O 3 @SOD and Mo/Al 2 O 3 Composite Catalyst

Kun Sun, Ge Yang, Jiaxin Han, Yongming Chai, Yanpeng Li, Chunzheng Wang, Svetlana Mintova, Chenguang Liu, Hailing Guo

▶ **To cite this version:**

Kun Sun, Ge Yang, Jiaxin Han, Yongming Chai, Yanpeng Li, et al.. Efficient Hydrodesulfurization of Dibenzothiophene over Core-Shell Ni/Al 2 O 3 @SOD and Mo/Al 2 O 3 Composite Catalyst. Inorganic Chemistry Frontiers, 2022, 9 (14), pp.3384-3391. 10.1039/D2QI00667G . hal-04295869

HAL Id: hal-04295869
https://hal.science/hal-04295869

Submitted on 20 Nov 2023

HAL is a multi-disciplinary open access archive for the deposit and dissemination of scientific research documents, whether they are published or not. The documents may come from teaching and research institutions in France or abroad, or from public or private research centers.

L'archive ouverte pluridisciplinaire **HAL**, est destinée au dépôt et à la diffusion de documents scientifiques de niveau recherche, publiés ou non, émanant des établissements d'enseignement et de recherche français ou étrangers, des laboratoires publics ou privés.

Efficient Hydrodesulfurization of Dibenzothiophene over Core-Shell Ni/Al_2O_3@SOD and Mo/Al_2O_3 Composite Catalyst

Kun Sun [a], Ge Yang [a,b,*], Jiaxin Han [a], Yongming Chai [a], Yanpeng Li [a], Chunzheng Wang [a], Svetlana Mintova [a,c], Chenguang Liu [a], Hailing Guo [a,*]

[a] State Key Laboratory of Heavy Oil Processing, College of Chemistry and Chemical Engineering, China University of Petroleum (East China), Qingdao 266580, PR China

[b] College of Science, China University of Petroleum (East China), Qingdao 266580, PR China

[c] Normandie University, CNRS, ENSICAEN, UNICAEN, Laboratoire Catalyse et Spectrochimie

E-mail: yangge@upc.edu.cn; guohl@upc.edu.cn

Abstract

One composite catalyst, consisting of a sulfur-tolerant Ni/Al_2O_3@SOD and a MoS_2/Al_2O_3, was developed for hydrodesulfurization of dibenzothiophene. The sulfur-resistant Ni/Al_2O_3@SOD core-shell catalyst was prepared by coating a Ni/Al_2O_3 core with a sodalite (SOD) shell via the gel hydrothermal method. The SOD shell (d = 0.3 nm) can block the entry of the smallest sulfur-containing molecules (hydrogensulfide d = 0.36 nm) while allow hydrogen molecules (d = 0.29 nm) diffuse to produce hydrogen spillover. With the excellent hydrogen spillover effect of the well-protected Ni, the composite catalyst (core-shell Ni/Al_2O_3@SOD-MoS_2/Al_2O_3) showed high catalytic activity and selectivity of the direct desulfurization pathway in the hydrodesulfurization (HDS) of dibenzothiophene. Compared with the composite catalysts (Pt/Al_2O_3@SOD-MoS_2/Al_2O_3) using noble metal Pt, the transition metal Ni composite catalyst exhibited broad hydrodesulfurization application prospects.

Keywords: core-shell, hydrogen spillover, sulfur-resistant, synergistic catalysis

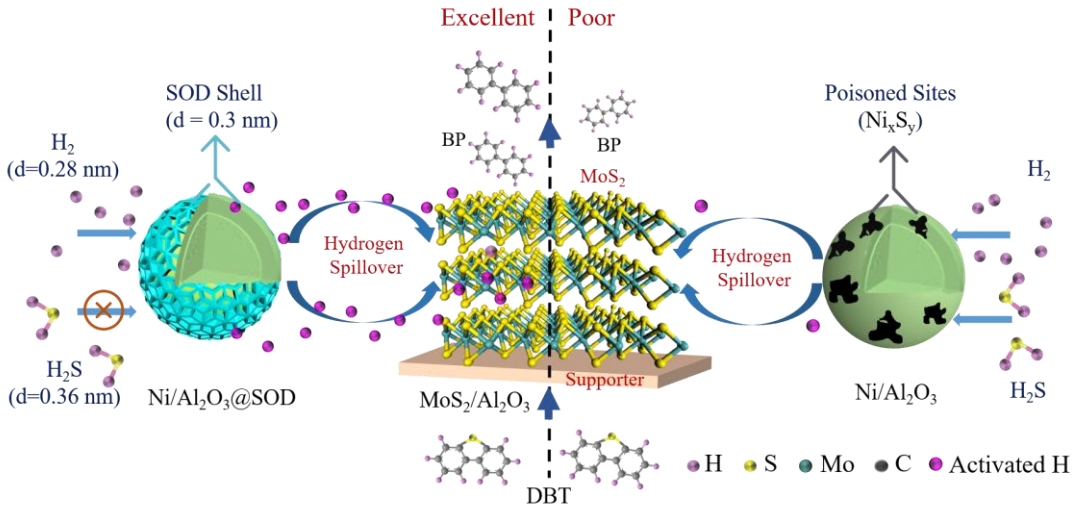

Scheme 1. The DBT HDS reaction scheme based on different composite catalyst (Ni/Al_2O_3@SOD-Mo/Al_2O_3 and Ni/Al_2O_3-Mo/Al_2O_3).

1.Introduction

The sulfur present in the transport fuels not only damages equipment but also poses an environmental hazard [1,2]. Therefore, the removal of sulfur compounds to obtain the ultralow sulfur fuels is always the focus in oil hydrorefining industry [3,4]. The transition metal Mo is widely applied in the hydrodesulfurization (HDS) reaction, which exhibits excellent HDS catalytic performance when being promoted by hydrogen spillover effect [5-8]. This high-performance enhancement phenomenon has prompted researchers to focus on the design and preparation of highly synergistic catalysts.

It is known that the hydrogen spillover refers to the phenomenon that activated hydrogen species adsorbed in the center of the solid catalyst (primary active center) migrate to other active centers (secondary active centers). Usually, the noble metals with suitable d-band holes, such as Ru, Rh, Pd, and Pt, can effectively dissociate hydrogen molecules into active hydrogen atoms or other ions (H^0, H^-, H^+, or H_2) and deliver them to the acceptor [9-11]. Thus, in the field of hydrodesulfurization (HDS), precious metals are widely applied as excitation base for hydrogen spillover [12,13]. However, the using of noble metals brings a huge economic burden for the realization of large-scale industrialization. Therefore, the development of an economical catalyst with excellent hydrogen spillover effect to assist Mo-based HDS catalysts, is of great significance for desulfurization industry.

In recent years, researchers have gradually verified that transition metals (Mn, Fe, Co, Ni, and Cu) also have the ability to activate hydrogen and generate hydrogen spillover [14-17]. Valdevenito et al. [18] applied the physically separated Ni//Mo catalyst in pyridine hydrodenitrogenation (HDN), and verified the existence of synergy between the bimetal catalysts and the positive effect of hydrogen spillover

effect triggered by Ni on the reaction. In the catalytic hydrodechlorination reaction, Claudia Amorima et al. [19] compared the performance of Pd/Al_2O_3 and Ni/Al_2O_3, indicating that transition metals also possess the ability to generate hydrogen spillover. While, the main challenge faced by transition metals is the threat of weakening the ability to activate hydrogen after being vulcanized by sulfur compounds in the HDS reaction [20-22].

One of the effective ways to protect metal from being vulcanized is adopting the core-shell concept [23, 24]. Herein, we chose the cheap transition metal Ni as the excitation source for hydrogen spillover, and prepared the Ni/Al_2O_3@SOD core-shell catalyst to provide active hydrogen species for MoS_2/Al_2O_3 in HDS of dibenzothiophene (DBT). By adjusting the thickness, pore size and chemical properties of the shell material, the SOD membrane was evenly coated on the surface of Ni/Al_2O_3 catalyst to protect the inner core active metal (Ni) from being poisoned relying on the molecular sieving effect. The performance of the Ni/Al_2O_3@SOD-MoS_2/Al_2O_3 composite catalyst for the hydrodesulfurization of dibenzothiophene (DBT) presented high activity, long lifetime and high pathway selectivity due to efficient hydrogen overflow effect trigged by Ni, and the catalytic effect is close to that of noble metal (Pt)-coupled catalysts. This synthesized Ni/Al_2O_3@SOD catalyst has greater economic value for the large-scale application in HDS industry.

2. Experimental

2.1 Chemicals

Carbamide (AR, 99%), n-heptane (AR, 97%), sodium hydroxide (AR), aluminium powder (AR, 99.5%), n-buty alcohol (AR, 99%), potassium bromide (AR, 99%), diphenylthiophene (AR, 98%), 4,6-dimethyldibenzothiophene (AR, 97%),

nickel nitrate hexahydrate (AR, 98%), cyclohexene (GC, 99.7%), carbon disulfide (AR, 98%), ammonium molybdate tetrahydrate (AR), and LUDOX AS-40 colloidal silica (40% SiO_2 in water) are all purchased from Macklin Reagent Co., Ltd. α-Al_2O_3 pellets (Sasol, 1-2 mm, 42.2 $m^2 \cdot g^{-1}$), γ-Al_2O_3 pellets (Sasol, 1-2 mm, 210 m^2/g), chloroplatinic acid, urea (AR, 99%) and citric acid monohydrate (GR, 99.8%) were purchased from Sinopharm chemical reagent Co., Ltd. China. Self-made Deionized water.

2.2 Preparation of Ni/Al_2O_3@SOD

a. The supported Ni/Al_2O_3 catalyst (named NA) can be synthesized through equal volume impregnation: Ni impregnation solution (Ni: 29.3 wt.%)： 14.5 g of nickel nitrate hexahydrate was dissolved in 10.0 mL of deionized water. 10 g α-Al_2O_3 pellets (high acid and alkali resistance and mechanical strength) were placed in the ziplock bag including the Ni impregnation solution (3 mL). The ziplock bag was shaked slightly until the Ni impregnation solution was adsorbed by the α-Al_2O_3 pellet completely (water suction rate: 30%). The immersed pellets were dried at room temperature for 10 hours, and then transferred to further drying at 120 °C for 20 hours. Finally, the samples were calcined in air at 500 ºC for 4 h. The Ni loading on the α-Al_2O_3 measured by inductive coupled plasma emission spectrometer (ICP) analysis was 8.0 wt.%.

b. The Ni/Al_2O_3@SOD catalyst was prepared as follows: the NA catalyst was surface-treated with 5 wt.% NaOH solution at 120 ºC for 2 h, and then washed with ethanol for four times for surface activation. The viscous SOD gel was prepared as described in part 1.1 of Supporting Information (SI). The surface-treated NA was evenly wrapped by the highly viscous SOD gel, and then transferred to a Teflon-lined autoclave at 60 ºC for 20 h. After rinsed with deionized water, the product was dried

in an oven at 120 ºC for 12 h to obtain the core-shell Ni/Al_2O_3@SOD catalyst (named NASOD).

2.3 Performance evaluation of catalysts

2.3.1 Hydrogenation (HY) activity and sulfur resistance *of Ni/Al_2O_3@SOD core-shell catalyst*

The catalytic hydrogenation (HY) activity evaluation was carried out to verify the sieving effect and sulfur resistance of as synthesized Ni/Al_2O_3@SOD core-shell catalyst. The mixture of n-heptane and 20 wt.% cyclohexene was selected as the raw material. The HY catalytic activity was evaluated in the temperature range 200-280 °C at 1 MPa, with 10 h^{-1} liquid hourly space velocity and 200 NL/L H_2/feedstock ratio. The Ni/Al_2O_3@SOD catalyst was activated (120 °C, 2 hours) and reduced (320 °C, 4 hours) in the reaction tube firstly. Then, after cooled to 200 °C, the liquid material was feuded. When the reaction reached stable, liquid samples were taken every two hours at a texting temperature point and analyzed using an Agilent 7890N PONA GC. The rate of all heating processes was 2 °C/min.

The sulfur resistance evaluation was carried out at 260 °C. The mixture of n-heptane, 20 wt.% cyclohexene and 2 wt.% carbon disulfide (CS_2) was chosen as the feeding material. The operating conditions were consistent with hydrogenation evaluation. After the activation and reduction process, the temperature was cooled to 260 °C and the liquid samples were collected every hour and analyzed using an Agilent 7890N PONA GC. The reaction lasted 18 hours.

2.3.2 HDS catalytic performance evaluation of composite catalyst

Mo-based catalyst (Mo/Al_2O_3) was selected as the main catalyst (the preparation of Mo/Al_2O_3 catalysts was listed in the part 1 of supporting information), and the core-shell catalyst (Ni/Al_2O_3@SOD) synthesized in this experiment was used as the

hydrogen spillover excitation site. The HDS evaluation was carried out over the composite catalyst (Ni/Al_2O_3@SOD-Mo/Al_2O_3) in a high-pressure fixed-bed reactor in the temperature range 240-300 ℃ at 2.0 MPa, with 3.0 h^{-1} LHSV and 300 NL/L H_2/feedstock ratio. The n-heptane solution containing 3 wt.% diphenylthiophene (DBT) and the mixture of DBT and 4,6-Dimethyldibenzothiophene (4,6-DMDBT) (the molar ratio of DBT and 4,6-DMDBT is 3:1) in n-heptane solution as the two desulfurization reactants, which the S content remains the same (S: 5208 ppm). After the activation and reduction part, the catalyst neeed to be pre-sulfided with 3 wt.% carbon disulfide (CS_2) dissolved in heptane at 300 ℃ for 6 h. Then the temperature decreased to 240 ℃ to start the HDS evaluation. The liquid samples were collected every 6 hours at every testing temperature, and analyzed using an Agilent 7890N PONA GC.

2.4 Characterization

Powder X-ray diffraction (XRD) patterns were collected on Bruker D8 Advance ($\lambda_{Cu\ K\alpha}$=1.5404 Å, 40 mA and 40 kV) with 15 º/min scanning step. X-ray photoelectron spectral (XPS) analysis was carried out using a PH 5000 Versaprobe system with a monochromatic Al Kα radiation (hν = 1486.6 eV) to determine the valence state of elements in the catalyst. All binding energies were calibrated related to the C 1s peak (284.6 eV). The reduction information of catalysts was determined by temperature programmed reduction (TPR) in the ChemBET3000 Chemisorption Analyzer (Quantachrome Instruments) from room temperature to 800 ℃ (heating rate 10 ℃/min), and the flow rate was 80 mL/min (H_2: 10% v/v). The inductively coupled plasma atomic emission spectrometer (ICP) was collected from Agilent`s ICP-OES 720ES. Agilent's 7890 Gas Chromatography was used for HY and HDS evaluation. The size and morphology of the catalysts were characterized using a transmission

electron microscope (TEM) at an operating voltage of 200 kV (JEOL JSM-3010) and a scanning electron microscope (SEM, JEOL-7900F). Energy dispersive spectroscopy (EDS) of the catalysts was performed on an EDAX XM2-30T apparatus.

3. Results and discussion

3.1 Characterization of core-shell Ni/Al_2O_3@SOD catalysts.

From Figure 1, both Ni/Al_2O_3@SOD and Ni/Al_2O_3 catalysts showed characteristic peaks of α-Al_2O_3 at 2θ =25.6°, 35.2°, 43.6° and 57.6° (JCPD`S 71-1123), indicating that the pretreated alumina support possessed perfect α-Al_2O_3 crystal. After loading nickel on the Al_2O_3 by impregnation method, it can be found that the Ni/Al_2O_3 (NA) and Ni/Al_2O_3@SOD (NAS) catalysts showed characteristic peaks of nickel oxidation state at 2θ =32.3°, 32.6°, 37.2° and 62.9° (JCPD`S 47-1049), indicating the effective load. In addition, the NAS catalyst coated with the SOD zeolite shell showed the SOD molecular sieve features at 2θ=14.0°, 23.9° and 32.1°, which confirmed that the formation of SOD type zeolite on the surface of the supported Ni/Al_2O_3 catalyst by the gel-hydrothermal method.

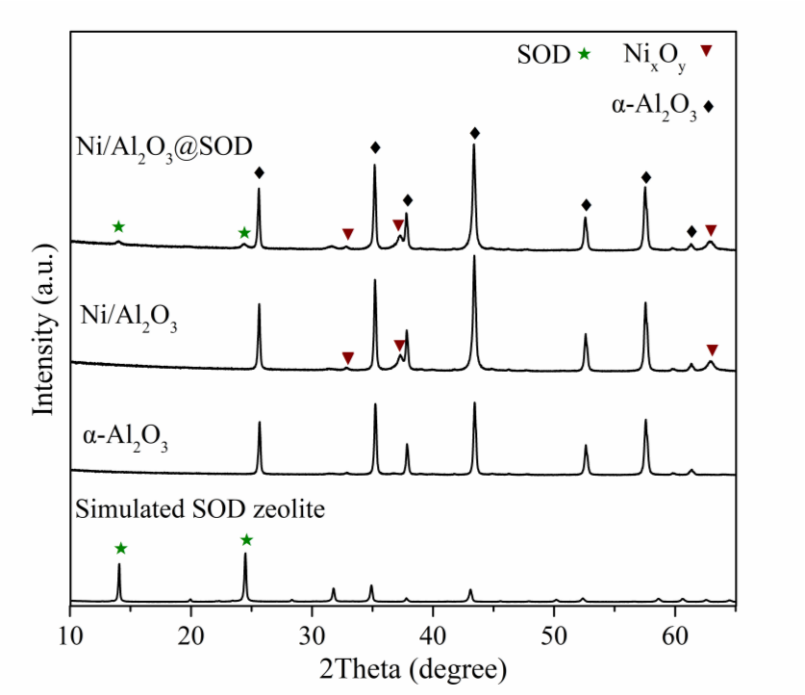

Figure 1. XRD patterns of core-shell catalysts.

The surface and cross-section morphology of Ni/Al_2O_3 catalyst and Ni/Al_2O_3@SOD core-shell catalyst were obtained by SEM. The porous structure of Ni/Al_2O_3 can be observed from both the surface and interface (Figure 2a, 2b). After being coated with the SOD zeolite, the surface of Ni/Al_2O_3@SOD (NASOD) presented a particle stacking state (Figure 2c). It can be clearly seen from the cross-sectional view (Figure 2d) that the thickness of the SOD membrane was about 10 μm, and compared with the inner core, the membrane layer had a tight texture and a high degree of intergrowth. No cracks, or shedding were observed at the interface of the SOD membrane and the inner core in Figure 2d. This reflected that the highly viscous SOD gel was more inclined to nucleate orderly, thus enhanced the force between core (Ni/Al_2O_3) and membrane (SOD), and ultimately promoted the formation of membrane with structural integrity, uniformity and controllable thickness.

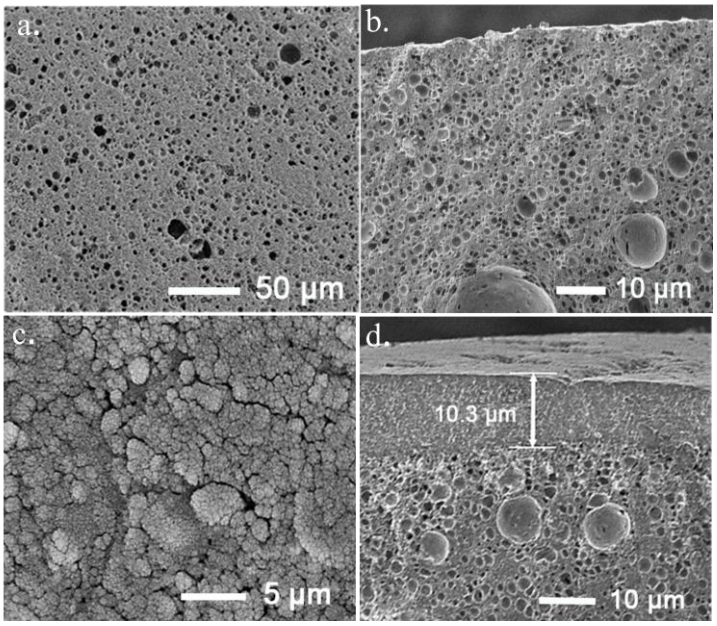

Figure 2. SEM images of cross section and surface of the Ni/Al_2O_3 (a. surface, b. cross section) and Ni/Al_2O_3 @SOD (c. surface d. cross section) catalysts.

The reducibility of Ni/Al_2O_3 (NA) and Ni/Al_2O_3@SOD (NASOD) catalysts was tested by H_2 temperature-programmed reduction (Figure 3). NA presented three distinct reduction peaks between 300 - 600 °C, which were related to the different steps in NiO reduction ($NiO \rightarrow Ni^{x+} \rightarrow Ni^0$) [25,26]. Among them, the peak around 315 °C was attributed to the reduction process of NiO particles exposed on the Al_2O_3 surface, and the other two peaks, located at 380 °C and 518 °C, were due to the reduction of small and larger NiO particles which were inside the Al_2O_3 supporter, respectively [27]. After being coated the SOD zeolite membrane (Ni/Al_2O_3@SOD catalyst), the reduction peaks temperature of the oxidized Ni generally became higher (342 °C, 430 °C, and 670 °C). It indicated that the SOD membrane had a certain shielding effect, which made the reduction of Ni more difficult. This also reflected the high degree of integration between the SOD membrane (shell) and the Ni/Al_2O_3 (inner core). In addition, the reduction peak area of NASOD catalyst was significantly smaller than that of NA, which was due to the less Ni exposure caused by the SOD membrane shell.

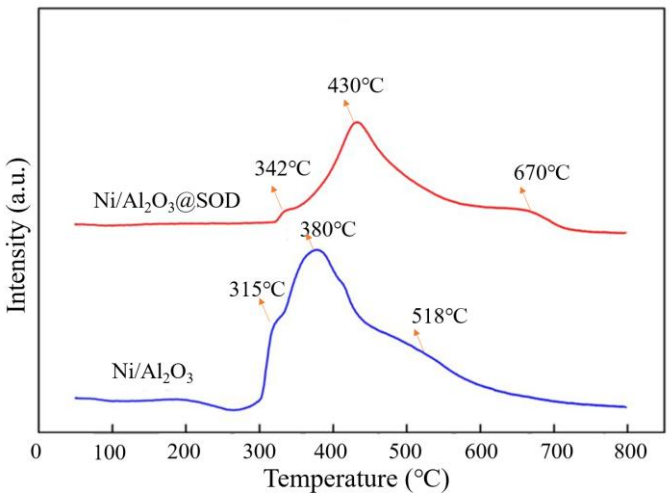

Figure 3. H_2-TPR profiles of Ni/Al_2O_3 and Ni/Al_2O_3@SOD catalysts.

3.2 Catalytic performance evaluation

3.2.1 Evaluation of sieving performance of SOD zeolite membrane

The cyclohexene hydrogenation reaction (HY) was used to verify the sieving effect of the core-shell structure. The NASOD catalyst (Ni/Al_2O_3@SOD) exhibited lower hydrogenation activity for cyclohexene than the NA catalyst (Ni/Al_2O_3) as shown in Figure 4a. This is because the dynamic diameter of cyclohexene molecule (0.42 nm) is larger than the pore size of the SOD zeolite (0.3 nm). Therefore, the cyclohexene molecules are blocked outside the SOD membrane and cannot contact the hydrogenation sites on Ni, in addition, the SOD molecular does not have hydrogenation sites [28, 29], which eventually leads to the low hydrogenation conversion of the NASOD catalyst. It also reflects the integrity and the screening effect of the SOD membrane coated on the Ni/Al_2O_3.

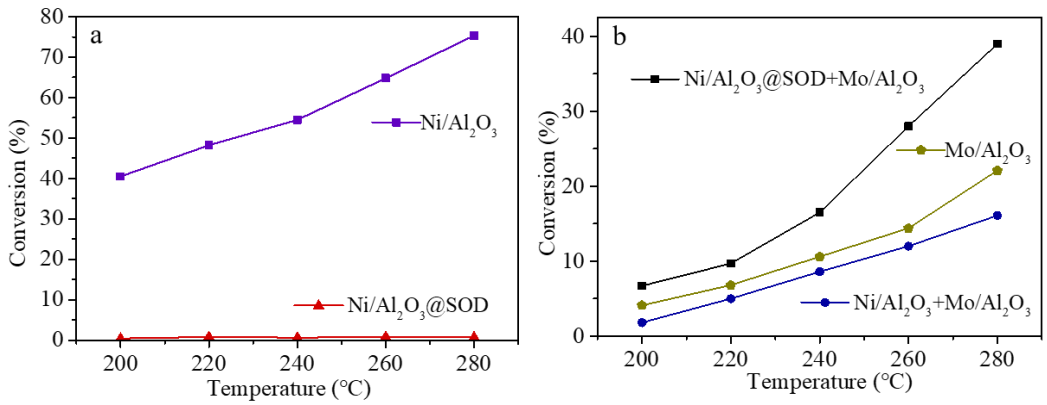

Figure 4. Conversion of the hydrogenation of cyclohexene over Ni/Al_2O_3, Ni/Al_2O_3@SOD, Ni/Al_2O_3@SOD-Mo/Al_2O_3, Ni/Al_2O_3-Mo/Al_2O_3 and Mo/Al_2O_3 catalysts.

The HY catalytic results of the two composite catalysts NASOD-M (Ni/Al_2O_3@SOD-Mo/Al_2O_3) and NA-M (Ni/Al_2O_3-Mo/Al_2O_3) were listed in Figure 4b (The synthesis and characterization of structure and properties about Mo/Al_2O_3 catalyst can be seen in the part 1.2 and part 2 of SI). The catalytic hydrogenation activity of the composite NASOD-M core-shell catalyst was significantly better than that of Mo/Al_2O_3. This can be explained by the hydrogen spillover remote control

model. In the catalytic process, H_2 (d = 0.28 nm) can freely pass through the shell SOD membrane (d = 0.30 nm) to contact with the Ni and be activated and dissociated. Then the numerous activated hydrogen molecules migrated to the hydrogenation site of MoS_2/Al_2O_3 catalyst relying on the hydrogen spillover effect, which improving the overall hydrogenation performance of the Mo/Al_2O_3 catalyst. Moreover, this also confirmed that the transition metal Ni possessed high hydrogen spillover excitation ability, and can be used as a cheap active hydrogen emission source for further large-scale application. Besides, it should be noted that the promotion effect was not observed in the composite NA-M catalyst. It was attribute to that the metal Ni in the NA-M catalyst had been poisoned during the pre-sulfide process of the evaluation without the protection of SOD membrane (d = 0.30 nm), and the obtained sulfide nickel had lower ability to activity hydrogen than metal Ni. This remarkably reflected that the transition metal Ni could play an excellent hydrogen spillover role after being well protected by the SOD membrane.

3.2.2 Sulfur resistance evaluation

In order to further verify the sieving and protecting performance of the SOD shell, the sulfur resistance evaluation was carried out. It can be known from the evaluation results (Figure 5), the Ni/Al_2O_3 catalyst was quickly sulfided and deactivated within the first 1 hour. After 7 hours, it was completely poisoned and lost its catalytic hydrogenation activity entirely. While, the catalytic activity of the NASOD-M composite catalyst (Ni/Al_2O_3@SOD-Mo/Al_2O_3) had maintained in a stable state and was higher than that of the NA-M composite catalyst (Ni/Al_2O_3-Mo/Al_2O_3). The fact apparently proved that the SOD membrane shell realized the sieving of sulfur-containing compounds, and effectively improved the sulfur resistance and catalytic stability of the metal catalyst.

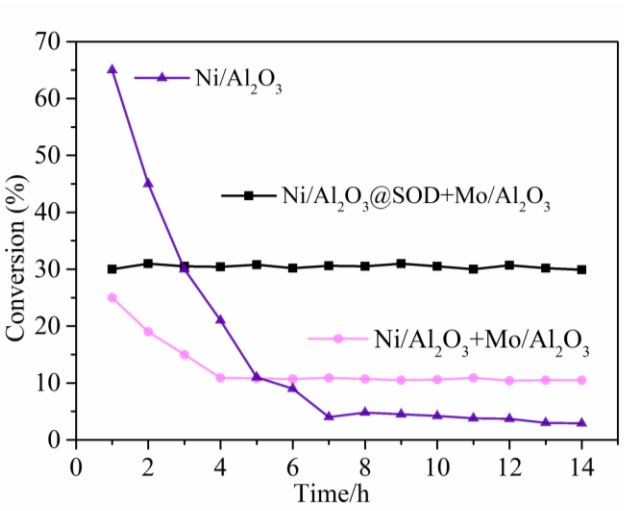

Figure 5. Evaluation of sulfur resistance of Ni/Al_2O_3, Ni/Al_2O_3@SOD-Mo/Al_2O_3, and Ni/Al_2O_3-Mo/Al_2O_3 catalysts at 260 ℃.

3.2.3 HDS catalytic performance evaluation

After ensuring the anti-sulfur function of the as synthesized core-shell catalyst, we further evaluated its HDS performance. It is well known that the sulfided Ni can utilize sulfur vacancies (d-electron configurations) to activate hydrogen [36], but the activation ability is much lower than that of metal Ni which actives species by the adsorption of hydrogen molecules. In the evaluation process (Figure 6), the composite NA-M catalyst (Ni/Al_2O_3-Mo/Al_2O_3) showed the lowest catalytic activity due to the poisoned metal Ni (sulfided to Ni_yS_x by S-containing compounds), and the HDS conversion rate of DBT at 340 °C was only 40%. Notably, the composite NASOD-M catalyst (Ni/Al_2O_3@SOD-Mo/Al_2O_3) protected by SOD membrane (H_2S, d = 0.36 nm) showed excellent catalytic performance at the same temperature, and DBT's HDS conversion rate can reach 71% at 340 °C.

Moreover, the reaction temperature required by the NASOD-M catalyst was 40 °C lower than that of Mo/Al_2O_3 catalyst when they achieved the same DBT conversion (49.8%). This indicated that with the synergistic effect of well-protected metallic Ni (hydrogen spillover), the overall catalytic activity of the composite

catalyst can be greatly improved and the energy consumption can be significantly reduced (Scheme 1). In addition, it was worth mentioning that the performance of NASOD-M catalyst was very close to that of noble metal catalyst (Pt/Al_2O_3@SOD-Mo/Al_2O_3: PASOD-M. The synthesis process of Pt/Al_2O_3@SOD is shown in part 1.3 of SI) throughout the evaluation process. Notably, at the high reaction temperature, the catalytic activity of NASOD-M catalyst was even better than that of PASOD-M catalyst as shown in Figure 6. This reflected the high economic advantages of the as-synthesized composite NASOD-M catalyst.

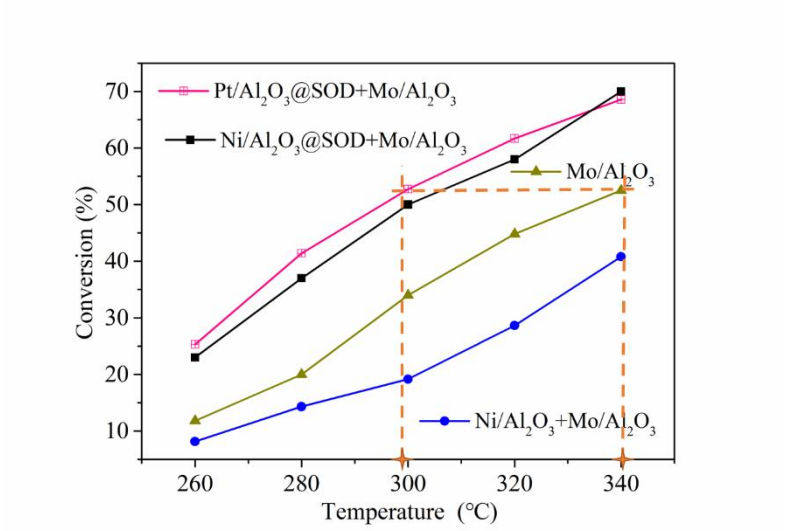

Figure 6. Conversion for the HDS of DBT over Mo/Al_2O_3, Ni/Al_2O_3@SOD-Mo/Al_2O_3, Pt/Al_2O_3@SOD-Mo/Al_2O_3, and Ni/Al_2O_3-Mo/Al_2O_3 catalysts.

In general, there are two reaction pathways for DBT in the HDS process [30,31]: one is the direct desulfurization pathway (DDS) to generate biphenyl (BP); another is the hydrodesulfurization pathway (HYD) which produce cyclohexylbenzene (CHB) and dicyclohexane (BCH) (Graph 1). According to analyzing the content ratio of BP and (CHB + BCH) in the product, the selectivity of the two HDS pathways can be obtained. We further evaluated the proportion of HDS reaction paths. It is known that the hydrodesulfurization (HDS) pathway of DBT over MoS_2 catalyst is mainly the

HYD pathway [31], and the proportion towards HYD is positively correlated with the reaction temperature. Therefore, the selectivity of DDS ($S_{DDS/HYD}$) decreased with the increase of reaction temperature (Figure 7). While, after adding the hydrogen spillover component to the catalyst (Ni/Al_2O_3@SOD), more active hydrogen was produced by the well - protected Ni as temperature rise. The numerous overflowing hydrogen reached the active sites on MoS_2, promoting the formation of SH-bonds and the removal of H_2S molecules, which leaded to the occurring of DDS route. Therefore, the Ni/Al_2O_3@SOD - Mo/Al_2O_3 catalyst exhibited higher DDS selectivity with increasing temperature.

It confirmed that the increasing of activated hydrogen was beneficial for its long-distance transmission and the occurrence of the DDS pathway in DBT HDS.

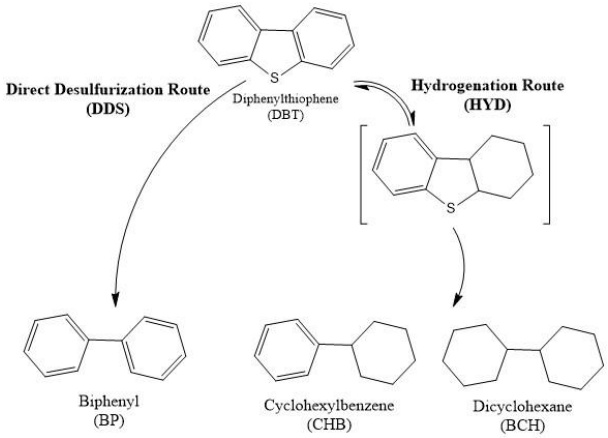

Graph 1. Two reaction routes of DBT hydrodesulfurization.

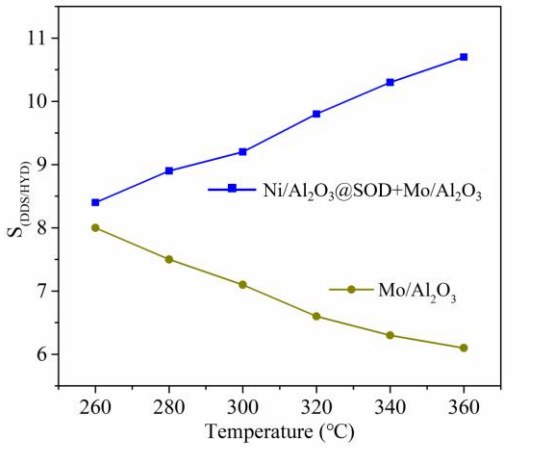

Figure 7. Selectivity of DBT HDS reaction pathway over Mo/Al_2O_3 and Ni/Al_2O_3@SOD-Mo/Al_2O_3 catalysts.

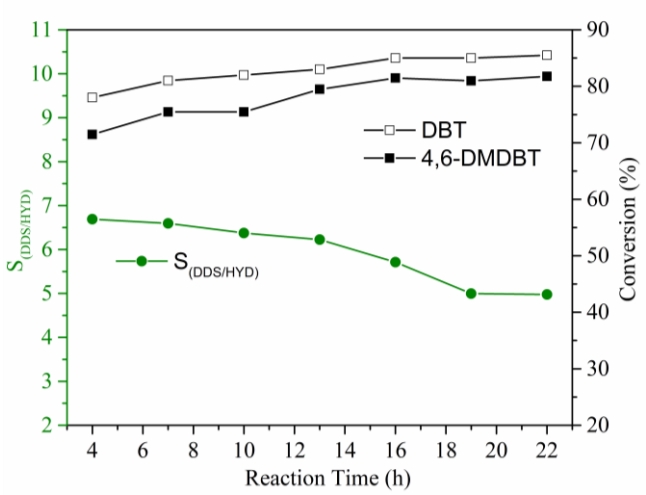

Figure 8. HDS conversion and reaction pathway selectivity of DBT and 4,6-DMDBT over Ni/Al_2O_3@SOD-Mo/Al_2O_3 catalysts.

Furthermore, the HDS performance of core-shell catalyst (Ni/Al_2O_3@SOD-Mo/Al_2O_3) for DBT and 4.6-DMDBT mixed feeding was also evaluated at 340 ℃. It is clearly found that catalyst Ni/Al_2O_3@SOD-Mo/Al_2O_3 showed good desulfurization performance for the two sulfides, and had good stability (Figure 8). However, the selectivity of the DDS pathway decreased slightly as the reaction proceeded. This is because in the stable stage of the catalyst (the first 8 hours), the removal of sulfur on DBT is the main reaction and the desulfurization route is the DDS pathway [32,33]. With the progress and stability of the reaction, the desulfurization rate of 4,6-DMDBT gradually increased, and its desulfurization route was dominated by the HYD pathway due to its huge steric hindrance effect [34,35]. The increase of the desulfurization rate of 4,6- DMDBT was greater than that of DBT, so the overall selectivity of the DDS pathway ($S_{(DDS/HYD)}$) decreased slightly. This also indicated that the SOD membrane can protect the metal Ni even in the environment with various sulfur-containing compounds, once again proving the

integrity of the core-shell structure.

Based on the above evaluation results, it can be seen that: 1. Well-protected metal Ni is an excellent and inexpensive active hydrogen excitation sites and has broader industrial large-scale application prospect; 2. Remote control synergy based on hydrogen spillover effect is an effective method to improve the catalysis activity and control the reaction path.

4. Conclusion

The SOD zeolite membrane shell of the Ni/Al_2O_3@SOD catalyst prepared by the gel hydrothermal method was combined tightly with the core (Ni/Al_2O_3). The zeolite membrane showed high degree of inter-particle intergrowth, realizing the controllable preparation of the zeolite membrane thickness. By coupling with the Mo/Al_2O_3 catalyst, the synergistic catalysis of transition metal Ni, the hydrogen spillover remote control model and the fence effect of SOD membrane were further explored. Conclusions as below: (1) The transition metal Ni with the protection of SOD membrane showed high synergistic catalytic ability. The complete development of the hydrogen spillover capability over transition metal Ni has greater economic value than the application of precious metals. (2) The hydrogen spillover remote control model was initially established, which can improve the HDS catalytic efficiency and reduce the reaction temperature. This Ni/Al_2O_3@SOD catalyst can greatly reduce energy loss, increase product revenue, and have broad industrial application prospects.

Acknowledgement

This work is supported by the National Natural Science Foundation of China (Gran No. U1862118, No. 22175200, No. 21975285, No.21991091, No. 21991090), the Fundamental Research Funds for the Central Universities (No. 21CX06024A),

and the Sino-French International Associated Laboratory LIA “Zeolite”.

Reference

[1] T.A. Saleh, S.A. AL-Hammadi, and A. Al-Amer, Effect of boron on the efficiency of MoCo catalysts supported on alumina for the hydrodesulfurization of liquid fuels, *Process.Saf. Environ.*, 2018, 121, 165-174.

[2] T.A. Saleh, Characterization, determination and elimination technologies for sulfur from petroleum: Toward cleaner fuel and a safe environment, *Trends Environ. Anal. Chem.*, 2020, 25, e00080.

[3] W. Lai, C. Zhou, J.P. Zhu, Y.L. Yang, J.B. Zheng, X.D. Ying, and W.P. Fang, A NiMoS flower-like structure with self-assembled nanosheets as high-performance hydrodesulfurization catalysts, *Nanoscale*, 2016, 8, 3823.

[4] O.Y. Gutiérrez, S. Srujan, E. Schachtl, J. Kim, E. Kondratieva, J. Hein, and J.A. Lercher, Effects of the Support on the Performance and Promotion of (Ni)MoS_2 Catalysts for Simultaneous Hydrodenitrogenation and Hydrodesulfurization, *Acs Catal.*, 2014, 4, 487-1499.

[5] L.V. Haandel, G. Smolentsev, J.A. Bokhoven, E.J.M. Hensen, and T. Weber, Evidence of Octahedral Co-Mo-S Sites in Hydrodesulfurization Catalysts as Determined by Resonant Inelastic X-ray Scattering and X-ray Absorption Spectroscopy, *ACS Catal.*, 2020, 10, 10978-10988.

[6] P.A. Nikulshina, D.I. Ishutenkoa, A.A. Mozhaeva, K.I. Maslakovb, and A.A. Pimerzin, Effects of composition and morphology of active phase of $CoMo/Al_2O_3$ catalysts prepared using Co_2Mo_{10}-heteropolyacid and chelating agents on their catalytic properties in HDS and HYD reactions, *J. Catal.*, 2014, 312, 152-169.

[7] F. Jiao, H.L. Guo, Y.M. Chai, H. Awala, S. Mintova, and C.G. Liu, Synergy between a sulfur-tolerant Pt/Al_2O_3@sodalite core–shell catalyst and a $CoMo/Al_2O_3$ catalyst, *J. Catal.*, 2018, 368, 89-97.

[8] S. Khoobiar, Particle to particle migration of hydrogen atoms on platinum—alumina catalysts from particle to neighboring particles, *J. Phys. Chem. C*, 1964, 68, 411-412.

[9] W. Curtis Conner Jr, and J.L. Falconer, Spillover in heterogeneous catalysis, *Chem. Re.v*, 1995, 95, 759-788.

[10] F. Roessner, and U. Roland, Hydrogen spillover in bifunctional catalysis, *J Mol*

Catal A-Chem., 1996, 112, 401-412.

[11] R. Prins, Hydrogen spillover. Facts and fiction, *Chem Rev.*, 2012, 112, 2714-2738.

[12] J.R. Chang, S.L. Chang, and T.B. Lin, γ-alumina-supported Pt catalysts for aromatics reduction: a structural investigation of sulfur poisoning catalyst deactivation, *J. Catal.*, 1997, 169, 338-346.

[13] L. Zhang, W.Q. Fu, Q.P. Ke, S. Zhang, H.L. Jin, J.B. Hu, S. Wang, and T.Tang, Study of hydrodesulfurization of 4,6-DM-DBT over Pd supported on mesoporous USY zeolite, *Appl. Catal. A: Gen*., 2012, 433, 251-257.

[14] P. Baeza, M.S. Ureta-Zañartu, N. Escalona, J. Ojeda, F.J. Gil-Llambías, and B. Delmon, Migration of surface species on supports: a proof of their role on the synergism between CoS_x or NiS_x and MoS_2 in HDS, *Appl. Catal. A: Gen*., 2004, 274, 303-309.

[15] J.H. Sinfelt, and P.J. Lucchesi, Kinetic evidence for the migration of reactive intermediates in surface catalysis, *J. Am. Chem. Soc.*,1963, 85, 3365-3367.

[16] L.H. Liu, B. Liu, Y.M. Chai, Y.Q. Liu, and C.G. Liu, Synergetic effect between sulfurized Mo/γ-Al_2O_3 and Ni/γ-γ-Al_2O_3 catalysts in hydrodenitrogenation of quinoline, *J. Energ. Chem.*, 2011, 20,214-217.

[17] B. Liu, L. Liu, Z. Wang, Y.M. Chai, H. Liu, C.L. Yin, and C.G. Liu, Effect of hydrogen spillover in selective hydrodesulfurization of FCC gasoline over the CoMo catalyst, *Catal. Today*, 2017, 282, 214-221.

[18] F. Valdevenito, R. García, N. Escalona, F.J. Gil-Llambias, S.B. Rasmussen, and A. López-Agudo, Ni//Mo synergism via hydrogen spillover, in pyridine hydrodenitrogenation, *Catal. Commun.*, 2010, 11, 1154-1156.

[19] C. Amori, and M.A. Keane, Catalytic hydrodechlorination of chloroaromatic gas streams promoted by Pd and Ni: The role of hydrogen spillover, *J. Hazard. Mater.*, 2012, 211-212, 208-217.

[20] J.C. McCarty, and H. Wise, Thermodynamics of sulfur chemisorption on metals. I. Alimina-supported nickel, *J. Chem. Phys.*, 1980, 72, 6332-6337.

[21] B. Pawelec, P.Castaño, J.M. Arandes, J. Bilbao, S. Thomas, M.A. Peña, and J.L.G. Fierro, Factors influencing the thioresistance of nickel catalysts in aromatics hydrogenation, *Appl. Catal. A: Gen*., 2007, 317, 20-33.

[22] P.J. Mangnus, E.K. Poels, A.D. van Langeveld, and J.A.Moulijn, Comparison of

the sulfiding rate and mechanism of supported NiO and Ni0 particles, *J. Catal.*, 1992, 137, 92–101.

[23]T. Tan, L.Zhang, W. Fu, Y.Ma, J. Xu, J. Jiang, G. Fang, and F.S. Xiao, Design and synthesis of metal sulfide catalysts supported on zeolite nanofiber bundles with unprecedented hydrodesulfurization activities, *J. Am. Chem. Soc.*, 2013, 135, 11437-11440.

[24] J. Im, H. Shin, H. Jang, H. Kim, and M. Choi, Maximizing the catalytic function of hydrogen spillover in platinum-encapsulated aluminosilicates with controlled nanostructures, *Nat. Commun.*, 2014, 5, 1-8.

[25] W.J. Shan, M.F. Luo, P.L. Ying, W.J. Shen,and C. Li, Reduction property and catalytic activity of $Ce_{1-X}Ni_XO_2$ mixed oxide catalysts for CH_4 oxidation, *Appl. Catal. A: Gen.*, 2003, 246, 1-9.

[26] D. Delgado, B. Solsona, A. Ykrelef, A. Rodríguez-Gómez, A. Caballero Orcid, E. Rodríguez-Aguado, E. Rodríguez-Castellón, and J. M. López Nieto, On the Redox and Catalytic Properties of Promoted NiO Catalysts for the Oxidative Dehydrogenation of Ethane, *J. Phys. Chem. C*, 2017,121, 25132-25142.

[27] C.T. Shen, Y.H. Lee, K. Xie, C.P. Yen, J.W. J, K.R. Lee, S.W. Lee, and C.J. T, Correlation between microstructure and catalytic and mechanical properties during redox cycling for Ni-BCY and Ni-BCZY composites, *Ceram. Int.*, 2017, 43, S671-S674.

[28] R. Prins, V. Pálfi, and M. Reiher, Hydrogen spillover to nonreducible supports, *J. Phys. Chem. C*, 2012, 116, 14274-14283.

[29] S. Garcia-Gil, D. Teillet-Billy, N. Rougeau, and V. Sidis, H atom adsorption on a silicate surface: The (010) surface of forsterite, *J. Phys. Chem. C*, 2013,117, 12612-12621.

[30] B.Liu, L. Liu, Z. Wang, Y.M. Chai, H. Liu, C.L. Yin, C.G. Liu, Effect of hydrogen spillover in selective hydrodesulfurization of FCC gasoline over the CoMo catalyst, *Catal. Today*, 2017, 282, 214-221.

[31] K. Sun, H.L. Guo, F. Jiao, Y.M. Chai, Y.P. Li, B. Liu, S. Mintova, C.G. Liu, Design of an Intercalated Nano-MoS2 Hydrophobic Catalyst with High Rim Sites to Improve the Hydrogenation Selectivity in Hydrodesulfurization Reaction, *Appl. Catal. B-Environ.*, 2021, 286, 119907.

[32] A.N.Varakin, A.V.Mozhaev, A.A.Pimerzin, P.A.Nikulshin, Comparable investigation of unsupported MoS_2 hydrodesulfurization catalysts prepared by different techniques: advantages of support leaching method, *Appl. Catal. B-Environ.*, 2018, 238, 498-508.

[33] B. Pawelec, R. Navarro, J. Camposmartin, J.G. Fierro, Towards near zero-sulfur liquid fuels: a perspective review, *Catal. Sci. Technol.* 2011, 1, 23-42.

[34] A.S. Walton, J.V. Lauritsen, H. Topsøe, F.Besenbacher, MoS_2 nanoparticle morphologies in hydrodesulfurization catalysis studied by scanning tunneling microscopy, *J. Catal.* 2013, 308, 306-318.

[35] P.A. Nikulshin, D.I. Ishutenko, A.A. Mozhaev, K.I. Maslakov, A.A.J.Jo.C. Pimerzin, Effects of composition and morphology of active phase of $CoMo/Al_2O_3$ catalysts prepared using Co_2Mo_{10}-Heteropolyacid and chelating agents on their catalytic properties in HDS and HYD reactions, *J. Catal.* 2014, 312, 152-169.

[36] H.J. Liu, W.L. Yu, M.X. Li, S.Y. Dou, F.L.Wang, R.Y. Fan, Y. Ma, Y.L. Zhou, Y.M. Chai, B. Dong, Rational Design of Ni_3S_2 Nanosheets-Ag Nanorods on Ni Foam with Improved Hydrogen Adsorption Sites for Hydrogen Evolution Reaction, *Sustain. Energy Fuels*, 2021,5, 3428-3435.